AGU ADVANCING EARTH AND SPACE SCIENCES

Geophysical Research Letters

RESEARCH LETTER
10.1029/2023GL104666

An Unprecedented Sea Ice Retreat in the Weddell Sea Driving an Overall Decrease of the Antarctic Sea-Ice Extent Over the 20th Century

Quentin Dalaiden[1], Jeanne Rezsöhazy[1], Hugues Goosse[1], Elizabeth R. Thomas[2], Diana O. Vladimirova[2], and Dieter Tetzner[2]

[1]Earth and Life Institute, Université catholique de Louvain, Louvain-la-Neuve, Belgium, [2]Ice Dynamics and Paleoclimate, British Antarctic Survey, Cambridge, UK

Quentin Dalaiden and Jeanne Rezsöhazy contributed equally to this work.

Key Points:

- The Antarctic sea-ice extent experienced a reduction over the 20th century
- The sea-ice extent in Weddell Sea reached its lowest level over the past 300 years at the end of the 20th century
- Models are unable to simulate the reconstructed sea ice increase in the Ross Sea, leading to an overestimation of the Antarctic sea ice loss

Supporting Information:

Supporting Information may be found in the online version of this article.

Correspondence to:

Q. Dalaiden,
quentin.dalaiden@uclouvain.be

Citation:

Dalaiden, Q., Rezsöhazy, J., Goosse, H., Thomas, E. R., Vladimirova, D. O., & Tetzner, D. (2023). An unprecedented sea ice retreat in the Weddell Sea driving an overall decrease of the Antarctic sea-ice extent over the 20th century. *Geophysical Research Letters*, *50*, e2023GL104666. https://doi.org/10.1029/2023GL104666

Received 24 MAY 2023
Accepted 7 OCT 2023

Author Contributions:

Conceptualization: Quentin Dalaiden, Jeanne Rezsöhazy, Hugues Goosse
Data curation: Elizabeth R. Thomas, Diana O. Vladimirova, Dieter Tetzner
Formal analysis: Quentin Dalaiden, Jeanne Rezsöhazy
Funding acquisition: Hugues Goosse
Writing – original draft: Jeanne Rezsöhazy, Hugues Goosse

Abstract Sea-ice extent is predicted to decrease in a warming climate. However, despite global warming over the past century, total Antarctic sea ice remained relatively stable from 1979 until 2015, before strongly melting. Here we explore the long-term sea ice variability by reconstructing Antarctic sea ice since 1700 CE, based on paleoclimate records and data assimilation. Our results indicate a decline in southern hemisphere sea-ice extent over the 20th century, driven by a reduction of 0.26 million km^2 in the Weddell Sea that reached values at the end of the century lower than any other reconstructed period. The Ross Sea experienced an increasing sea-ice cover trend due to a low-pressure system located off the Amundsen Sea coast, offset by a decreasing trend in the Bellingshausen-Amundsen Sea. Models failed to account for the Ross Sea increase, resulting in an overly uniform estimate of Antarctic sea ice loss over the 20th century.

Plain Language Summary Despite global warming, the Antarctic sea-ice extent remained relatively constant over the satellite era until 2015 before a strong reduction. Numerous studies analyzed this intriguing behavior but no consensus emerged, mainly because of the shortness of observations. Here, we reconstruct the Antarctic sea-ice over the past 300 years based on paleoclimate observations, in particular ice-core records, combined with the physics of climate models using a so-called data-assimilation technique. We show that there has been a decline in the Antarctic sea-ice extent during the 20th century. Specifically, the Atlantic sector displays a significant sea-ice extent reduction, reaching its lowest level at the end of our reconstruction compared to the past three centuries. Our results indicate sea-ice extent trends over the 20th century of variable signs in the Pacific sector, with a sea ice increase in western Pacific while a decrease is noticed in western Pacific. These heterogeneous spatial changes are mainly related to changes in the low-pressure system located off the West Antarctic coasts. According to our analysis, climate models are not able to simulate the observed sea ice expansion in the eastern Pacific, leading to a too large and too homogenous Antarctic loss during the 20th century.

1. Introduction

Sea ice is a key element of the climate system at high southern latitudes that controls the exchanges of energy, water and CO_2 between the ocean and atmosphere (Hobbs et al., 2016). Changes in sea-ice extent drive both regional and global ocean circulation and influence the melting of the Antarctic Ice Sheet (Caillet et al., 2023; Kusahara et al., 2019). Despite significant progress to document the sea ice dynamics over the last decades along with its interannual variability (Hobbs et al., 2016; Roach et al., 2022), uncertainties remain. While the shape of the seasonal cycle of the Antarctic sea-ice extent is mainly controlled by the seasonal cycle of insolation (Roach et al., 2022), atmospheric circulation plays a dominant role in the year-to-year variability at regional scale (P. R. Holland & Kwok, 2012; Hobbs et al., 2016; Kusahara et al., 2019). This is partly related to large-scale modes of atmospheric variability such as the Southern Annular Mode (SAM), which represents the strength and position of westerly winds, and El-Niño Southern Oscillation (ENSO) which have a large imprint on the spatial patterns of sea ice variability (Hobbs et al., 2016; Lefebvre & Goosse, 2005; Stammerjohn et al., 2008).

Over the satellite era, a slight positive trend in Antarctic sea-ice extent has been observed between 1979 and 2015, before a marked decrease over the last few years (Parkinson, 2019), with considerable emphasis placed on the extremely low sea-ice extent during recent years (Turner et al., 2022). Atmospheric modes of variability are associated with positive and negative anomalies of sea-ice extent in different regions, so their impacts on the total

Writing – review & editing: Quentin Dalaiden, Hugues Goosse, Elizabeth R. Thomas, Diana O. Vladimirova, Dieter Tetzner

sea-ice extent and their trends are not clear (Polvani et al., 2021). Oceanic feedback, connections with the tropics and the meltwater fluxes from the Antarctic Ice Sheet may also have contributed to the observed trends (Hobbs et al., 2016; Rye et al., 2020). Earth System Models generally simulate a decrease in sea-ice extent in response to the increase in atmospheric greenhouse gas concentration and thus fail to reproduce the observed trend over the past decades (Roach et al., 2020). However, it is unclear if the models overestimate the response of the Southern Ocean to the anthropogenic forcing or if internal variability may be large enough to mask the forced trend simulated by the models (Polvani & Smith, 2013; Roach et al., 2020; Zunz et al., 2013).

While our knowledge of Antarctic sea ice change over annual to decadal timescales is improving, our understanding of Antarctic sea ice variability at multi-decadal to centennial timescales remains very low, mainly because continuous satellite observations, that provide the main source of information on the evolution of the sea-ice concentration, are only available from the late 1970s. Based on instrumental surface air temperature and sea-level pressure observations, along with climate indices in the mid-latitudes of the southern hemisphere, a recent reconstruction of sea-ice extent in the different sectors of the Southern Ocean suggests a sea-ice extent decrease over the first half of the 20th century, followed by an increase in the second half (Fogt et al., 2022) (hereafter Fogt22). The shift occurred around the 1960s, that is, more than a decade before the start of regular satellite observations. This general picture is consistent with many independent estimates based on Antarctic expeditions (Edinburgh & Day, 2016; Titchner & Rayner, 2014), whaler's observations (De La Mare, 1997), fast ice records (Murphy et al., 2014a), sea ice reconstructions derived from ice-core records (Abram et al., 2010; Curran et al., 2003; Thomas & Abram, 2016) and climate models constrained by 20th century observations (Goosse et al., 2009). Some of those estimates provide local information during specific seasons, and many may suffer from large uncertainties, but all the evidence converges toward an overall sea-ice extent decrease before the 1960s, with some regional variations.

Several hypotheses, related to a possible role of wind changes, modification of the deep convection in the Southern Ocean, the stratospheric ozone depletion or the teleconnections with the tropics, have been proposed for changes in sea-ice extent over the 20th century but no convincing explanation is currently available (Goosse et al., 2009; Fan et al., 2014; L. Zhang et al., 2019; Fogt & Connolly, 2021; Fogt et al., 2022; Schneider & Deser, 2018; Landrum et al., 2017). Over longer timescales, sea ice reconstructions from marine sediment cores suggest the influence of the SAM and ENSO is maintained over the past millennium (Crosta et al., 2021). However, the sparsity of marine records, and their low sampling resolution, prevent us from obtaining a consistent picture prior to the 20th century (Thomas et al., 2019). Therefore, it is crucial to provide longer time-series of the historical Antarctic sea-ice extent to quantify the contribution of natural and forced variability in the observed changes. This could ultimately provide a physical explanation of the recent changes in concert with a more comprehensive picture of the issues of the models in reproducing the Antarctic sea ice changes over the satellite area, such as a potential underestimation of multi-decadal variability in models.

We describe here such a reconstruction using paleoclimate data assimilation (Hakim et al., 2016) covering the period 1700–2000 CE at annual resolution. Data assimilation has been applied in several recent studies to reconstruct climate variations at high southern latitudes (Dalaiden et al., 2021; O'Connor et al., 2021). In this study, we expand the suite of paleoclimate archives in the data assimilation to include a new compilation of ice-core sodium records covering the past 2000 years (Thomas et al., 2022). This provides skilful sea ice reconstruction over a longer period and a larger fraction of the Southern Ocean compared to previous attempts. A strong advantage of data assimilation compared to other techniques is the joined reconstruction of several variables at the same time, in a physically consistent way. This allows investigation of the physical mechanisms responsible for the changes, specifically here the potential role of changes in atmospheric circulation and winds on the sea-ice extent.

2. Methods and Data

2.1. Data Assimilation Method

The objective of paleoclimate data assimilation (DA) is to optimally combine models and proxy observations to estimate historical climate variations (Goosse et al., 2010; Hakim et al., 2016; Widmann et al., 2010). DA employs a Bayesian framework (van Leeuwen, 2009), where a range of states of the climate system is first obtained from an ensemble of climate model simulations (referred to as the prior). DA then aims at generating as accurate as possible reconstructions of the state of the climate system by updating this prior based on model

10.1029/2023GL104666

results using available proxy observations. A large benefit of DA is to spread the information from the proxy locations into space but also into variables that are not assimilated, by relying on the covariance between variables provided by the climate model. DA-based reconstructions thus guarantee dynamical consistency among all the reconstructed variables.

The DA method employed in this study follows an offline (or non-cycling) approach, where existing climate model simulations are used to construct the prior distribution (Hakim et al., 2016; Steiger et al., 2017). The model simulations selected for our data assimilation-based reconstructions are made up of the three simulations of the isotope-enabled Community Earth System Model version 1 (iCESM1) (Brady et al., 2019; Stevenson et al., 2019) covering the 850–1850 CE period. Those simulations have been selected as it is the only available ensemble with an isotope-enable model over the past millennium. Such an ensemble is needed here to have enough particles to avoid degeneracy of the particle filter (Dubinkina et al., 2011) (typically here more than 1,000 particles; Figure S1 in Supporting Information S1).

The method is based on a particle filter (Dubinkina et al., 2011), with an implementation identical to several recent studies (Dalaiden et al., 2021; Klein et al., 2019; Rezsöhazy et al., 2022). In the offline version of the particle filter, all the years of the model simulations constitute our prior as the years are assumed to be independent (referred to as particles), which is a reasonable assumption for the variables of interest (Brennan et al., 2020; Hakim et al., 2016; Matsikaris et al., 2015; Okazaki et al., 2021; Steiger et al., 2017). Given that the assimilated proxies are annually resolved (see Section 2.2), the DA procedure operates on an annual time step. Consequently, the prior distribution consists of annually averaged variables and contains both the assimilated and the target reconstructed variables. Since the prior remains fixed throughout the DA process, the temporal variability of the reconstruction only comes from the assimilated proxies.

During the reconstruction process, the prior is compared with the available observations for each year of the reconstructed period via a proxy system model (PSM) that relates the model variables to the observed quantity (see Section 2.3). Based on the difference between the model results and observations at that time, and taking into account the uncertainties related to the model and proxies (see Supplements), each particle receives a weight proportional to its likelihood knowing the observations. Particles close to observations receive a large weight; particles far away from observations receive a small weight. The mean reconstruction is then given by the weighted mean of the particles, and the range of the weighted ensemble provides a measure of the uncertainty of the reconstruction.

2.2. Paleoclimate Observations

The paleoclimate (or "proxy") records selected for the data assimilation are derived from ice-core and tree-ring archives. As in Dalaiden et al. (2021), it includes 46 snow accumulation records from Thomas et al. (2017a), one additional snow accumulation record (i.e., the B40 record) from Medley et al. (2018), 33 ratio of stable isotopes oxygen ($\delta^{18}O$) records from Stenni et al. (2017a) in ice cores and 12 tree-ring records in the Southern Hemisphere, three being located in New Zealand, three in Tasmania and six in South America from the PAGES2k database (PAGES2k Consortium et al., 2013; Emile-Geay et al., 2017a).

Additionally, in this study, we have also assimilated sodium records in Antarctic ice cores from a recent compilation (Thomas et al., 2022). We have chosen to use the sodium fluxes and not the sodium concentration as they have a better correlation with observations with winds over the satellite period (Thomas et al., 2022). For all the 67 sodium flux records, we kept only the ones covering at least 70% of the 20th century, in order to include a period that is long enough for our reconstructions. Furthermore, the records must have at least 20 years of data on the 1979–2019 CE period for the calibration. We finally end up with 17 records of sodium flux. Figure S2 in Supporting Information S1 displays all locations of proxy records.

2.3. Proxy System Models

As in Dalaiden et al. (2021), nearby ice-core records are grouped to reduce local noise and enhance the climatic signal in observations. In practice, records included in 500 km grid cells are averaged, resulting in composites. In order to perform the model-data comparison, we must derive from model results the variable that is observed, at the same location as it was measured. This is done through an observation operator or proxy system model

(Evans et al., 2013). It is performed in a simple way for δ^{18}O and snow accumulation as iCESM1 simulates δ^{18}O of precipitation and the amount of snowfall minus evaporation and sublimation over the continent. We assume here that those two variables can be directly compared to observations and include all additional processes, such as post-deposition effects, in the estimate of the error (Münch & Laepple, 2018).

As iCESM1 does not directly simulate sodium fluxes or tree growth, statistical proxy system models have been developed for those variables. They are based on a linear regression with the ERA5 atmospheric reanalysis (Hersbach et al., 2020a). As we assume that most of the sodium fluxes are mainly influenced by the atmospheric circulation (Legrand & Mayewski, 1997; Mayewski et al., 2017), each composite is first correlated with the ERA5 500-hPa geopotential height over 1979–2019 CE. The grid cell with the highest correlation coefficient in a 1,500 km radius (to approximately account for the size of the 500 km grid) is then identified. The explanatory variable corresponds to the area-mean of the ERA5 500-hPa geopotential height on the circle of 500 km radius centered on the highest correlation grid cell previously identified. The regression parameters are then calibrated over the 1979–2019 CE period using the ordinary least squares method. We then checked for consistency that the composites are significantly correlated with the explanatory variable (p-value < 0.1) and this is well the case for the 11 sodium flux composites. Sodium ice-core records are thus assimilated as 500-hPa geopotential observations. For the tree-ring width records, the proxy system models have been built with a uni- or bi-variate linear model on near-surface air temperature and/or precipitation variables (annual or seasonal) using the ordinary least squares method (see Dalaiden et al. (2021) for more details).

3. Results

3.1. Antarctic Sea Ice Reconstruction Over the Past Centuries

The data assimilation-based reconstruction provides the spatial distribution of several variables, at the resolution of the climate model prior but we will discuss here only the sea-ice concentration, as this is the focus of this study, and the sea-level pressure, as a measure of atmospheric circulation changes over the past centuries.

The sea-ice extent has been computed for five sectors of the Southern Ocean (Raphael & Hobbs, 2014) by integrating the ocean surface covered by at least 15% of ice (Figure 1). The reconstruction is significantly correlated (p-value < 0.05) with satellite observations over 1979–2000 CE and provides a skilful estimate, defined here as a positive Coefficient of Efficiency, for all sectors except for King Hakon (15°W–70°E; Table S1 in Supporting Information S1). The inclusion of sodium records enhanced the accuracy of our sea ice reconstruction compared to a previous study that did not utilize sodium records (Dalaiden et al., 2021) (Figure S2 and Table S2 in Supporting Information S1). This improvement is particularly noteworthy in the Weddell Sea and Ross Sea regions. Most sodium records are located in West Antarctica, explaining this improvement in these regions. Additionally, including sodium records allow us to extend the reconstructed period by 100 years. More generally, the performance of the sea ice reconstruction is poor in the Indian sector (0°W–90°E) (Figure S3 in Supporting Information S1), likely because of the small number of records available from East Antarctica (Figure S2 in Supporting Information S1). The highest correlation coefficients are obtained for the two sectors with the largest extent, the Weddell Sea sector (70°W–15°W), and the Ross Sea sector (165°–250°E) with values of 0.59 and 0.62 respectively (p-value < 0.05). In these two sectors, the correlation coefficient remains high and significant even when using only the longest records (Table S1 in Supporting Information S1). However, for the other sectors, the correlations decrease when using only the longest records, indicating a decrease in the skill of the reconstruction prior to 1850 (Table S1 in Supporting Information S1). Additionally, removing the linear trend before computing the correlation leads to very similar results, indicating that our skill over the instrumental era primarily comes from interannual variability.

Unlike Fogt22, which is calibrated using those satellite observations, our methodology uses no direct information on the observed state of the sea-ice extent. This provides a reconstruction that is totally independent of the satellite observations, but this naturally results in lower correlations with those observations than that of Fogt22. Nevertheless, the correlation with Fogt22 in the Weddell Sea is high over the whole 20th century, with a correlation coefficient reaching 0.63 (Figure 1). Our reconstruction also displays good agreement with an independent sea ice reconstruction in the northern Weddell Sea (Murphy et al., 2014a) (Figure S4 in Supporting Information S1). This indicates a strong consensus on the evolution of the sea-ice extent in the Weddell Sea over the 20th century showing a significant decrease of 0.25 million km^2 in one century (Table 1; 0.259 ± 0.031 and 0.245 million km^2

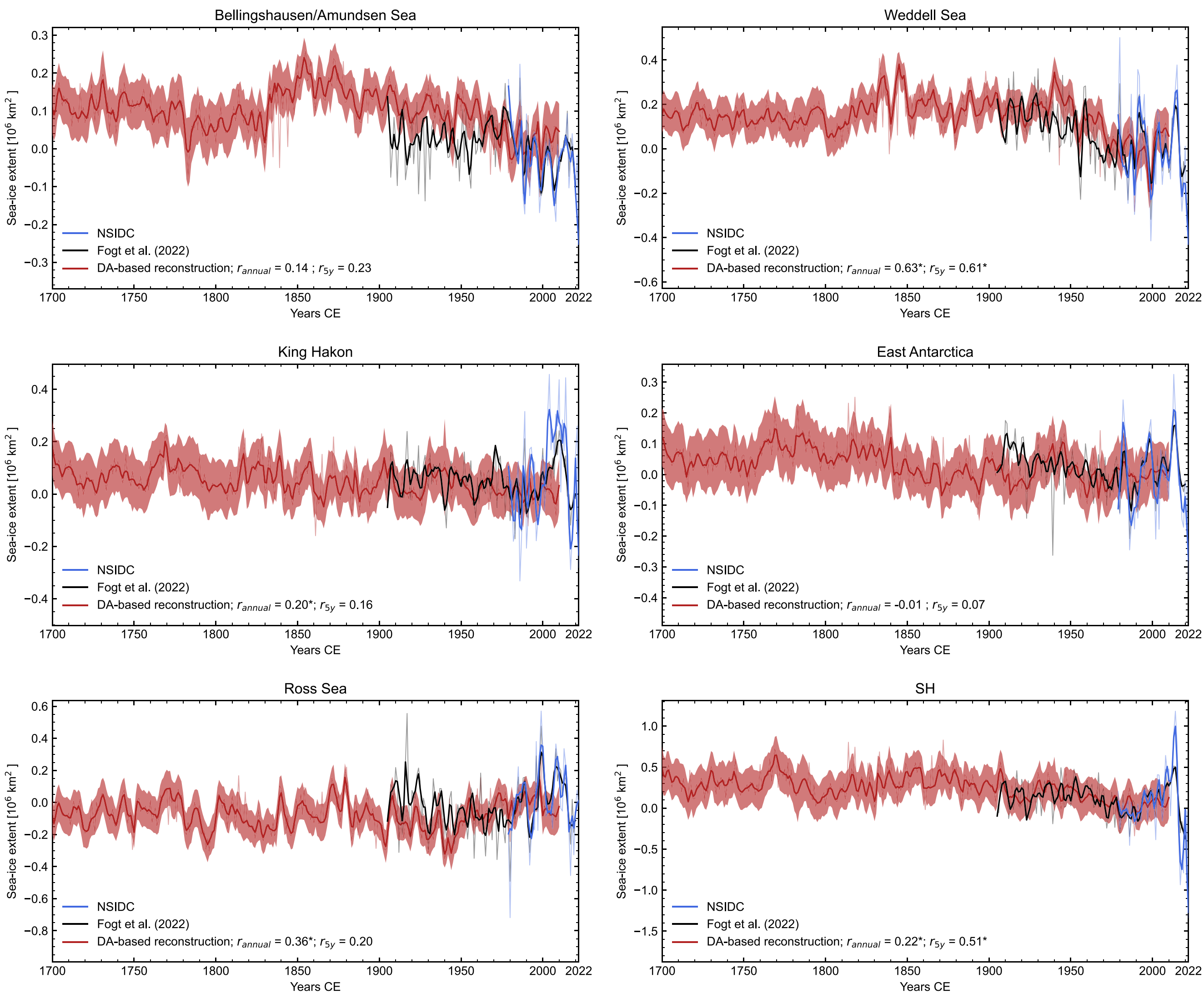

Figure 1. Time series of anomalies of sea-ice extent for the main Antarctic regions and pan-Antarctic (in 10^6 km^2). Anomalies are relative to the 1979–2000 CE period. Red curves represent our DA-based reconstruction while black curves are the reconstructions from Fogt et al. (2022) and blue curves correspond to satellite-derived observations (Parkinson, 2019). Thin and thick lines are annual and 5-yr mean (lowess smoothing), respectively. Shading represents the standard deviation of the ensemble mean from our DA-based reconstruction. Annual and 5-yr correlation coefficients between our DA-based reconstruction and the one from Fogt et al. (2022) are displayed (the smoothing is taken into account when calculating the statistical significance). Stars indicate statistically significant correlation (95% confidence). The regions are defined following Raphael and Hobbs (2014): the Bellinghausen/Amundsen Sea sector (110°–70°W), the Weddell Sea sector (70°–15°W), the King Hakon sector (15°W–70°E), the East Antarctica sector (70°–165°E) and the Ross Sea sector (165°–250°E). We also consider the Southern Hemisphere (SH) as a whole.

for our reconstruction and Fogt22, respectively), despite strong multi-decadal variability. The decreasing sea-ice extent trend in the Weddell Sea is also consistent with the analyses of early Antarctic expeditions (Titchner & Rayner, 2014) that display a retreat of the summer sea-ice extent of more than 1° in latitude between the 1897–1917 CE and 1989–2014 CE periods. Our longer reconstruction allows to put those 20th century changes in a longer context and indicates that values at the end of the 20th century are the lowest for the past three centuries.

In the Bellingshausen-Amundsen sector our reconstruction indicates a 20th century sea ice retreat (-0.153 ± 0.007 million km^2), while in the Ross Sea, we observe a sea-ice extent increase (0.199 ± 0.015 million km^2), in agreement with the dipole pattern obtained in a recent synthesis based on a large selection of sea ice reconstructions (Thomas et al., 2019), as well as with independent regional reconstructions based on the Methanesulfonic acid (MSA) content of nearby ice cores (Figure S4 in Supporting Information S1). By contrast, Fogt22 suggests a small decrease in the sea-ice extent in both the Bellingshausen-Amundsen and Ross sectors over that period. Sea ice anomalies are generally anti-correlated between these two sectors due to the atmospheric circulation in the

Table 1
Regional 20th Century Trends of Regional Sea-Ice Extent (in 10^6 km^2 per Century) in the Reconstruction of Fogt et al. (2022) (Fogt et al., 2022), Our DA-Based Reconstruction (the Uncertainty Is Estimated as the Interquartile Range of the Posterior), PMIP3 Mean and CESM1 Mean (the Numbers in Brackets Correspond to the Range of the Ensemble)

	DA-based reconstruction	Fogt et al. (2022)	PMIP3 mean	CESM1 mean
Bellingshausen/Amundsen Sea	−0.153 ± 0.007*	−0.019	−0.09* [−0.214;0.101]	−0.094* [−0.257;−0.005]
Weddell Sea	−0.259 ± 0.031*	−0.245*	−0.252* [−0.668;−0.049]	−0.262* [−0.421;−0.112]
King Hakon	−0.055 ± 0.034*	−0.069*	−0.417* [−1.098;−0.027]	−0.512 [−0.694;−0.288]
East Antarctica	−0.019 ± 0.004*	−0.069	−0.423* [−0.825;0.044]	−0.392 [−0.472;−0.305]
Ross Sea	0.199 ± 0.015*	−0.032	−0.222* [−0.372;0.068]	−0.220 [−0.499;−0.011]
SH	−0.287 ± 0.076*	−0.184*	−1.404* [−2.818;−0.242]	−1.479 [−2.039;−0.938]

Note. Asterisks indicate statistically significant trends at 95% level.

Amundsen Sea (Dalaiden et al., 2021; Hobbs et al., 2016). Due to this compensation, when integrating the trends over the two sectors, the total 20th century trend from Fogt22 and our reconstruction is very similar. Although relatively low for the Bellingshausen-Amundsen, the reconstructed values at the end of the 20th century remain in the range of the past 300 years for those sectors.

The total sea-ice extent in the Southern Ocean decreased by 0.287 ± 0.076 million km^2 over the 20th century (i.e., 2.9% per century), a value very close to the value for the Weddell Sea (0.259 ± 0.031 million km^2). A large multi-decadal variability is superimposed over the long-term negative trend. The sea-ice extent decrease occurred mainly between 1940 and 1980 CE, after which it stabilized at a consistently low level. This is in agreement with satellite observations and Fogt22. Our results thus indicate that the starting of satellite observations has been preceded by a large decrease in sea-ice extent. Reconstructing the sea-ice extent over the whole Southern Ocean is notoriously more difficult than locally because of strong and contrasting regional changes. However, our reconstruction of Antarctic sea-ice extent and Fogt22 are also significantly correlated over the 20th century, with a coefficient higher than 0.5 after a 5-yr smoothing (Figure 1), increasing the confidence in this result.

3.2. Changes in Atmospheric Circulation

In addition to providing a sea ice reconstruction, the data assimilation framework allows us to investigate the dynamical relationship with other variables, in particular wind changes. Our reconstruction of the sea-level pressure is skilful over most of the Southern Ocean, with the best performance in the Atlantic and Pacific sectors (Figure S3 in Supporting Information S1). The reconstruction of the SAM index is significantly correlated with the index obtained from instrumental data (G. J. Marshall, 2003) and in good agreement with previous reconstructions over the period 1700–2000 CE (Figure S5 in Supporting Information S1), with for instance a correlation with Dätwyler et al. (2018) that reaches 0.55 (p-value < 0.05) for 5-yr smoothed series. Our reconstruction is not independent of theirs as we share some of the proxy times-series as input but the methodology is totally different since the previous reconstructions used a regression-based approach. Compared with the Dalaiden et al. (2021) reconstruction, the wind reconstruction is improved in the Weddell Sector, in line with enhanced skill in that region for sea ice.

The SAM is the dominant mode of atmospheric variability of the extra-tropical circulation in the Southern Hemisphere. Therefore, the SAM index provides information on many elements of the southern hemisphere climate. However, sea-ice extent in the various sectors is mainly controlled by regional atmospheric patterns, which are themselves connected with large-scale variations (Hobbs et al., 2016; Raphael & Hobbs, 2014) (Figure S6 in Supporting Information S1). Specifically, during the 19th century, we observe sea-ice expansion in the Bellingshausen-Amundsen and eastern part of the Antarctic Peninsula, which might be caused by the cyclonic circulation anomaly located west of the Drake Passage bringing cold air from the continent to the Bellingshausen-Amundsen Sea (Figure 2). In contrast, a sea-ice extent decrease in the Weddell and Bellingshausen-Amundsen sectors combined with the increase in the Ross Sea over the 20th century is noticed. This can be explained in our reconstructions by a decrease in the sea-level pressure in the West Pacific Sector. This sea-level pressure decrease is consistent with the strengthening trend in the Amundsen Sea Low, a low-pressure system whose center of

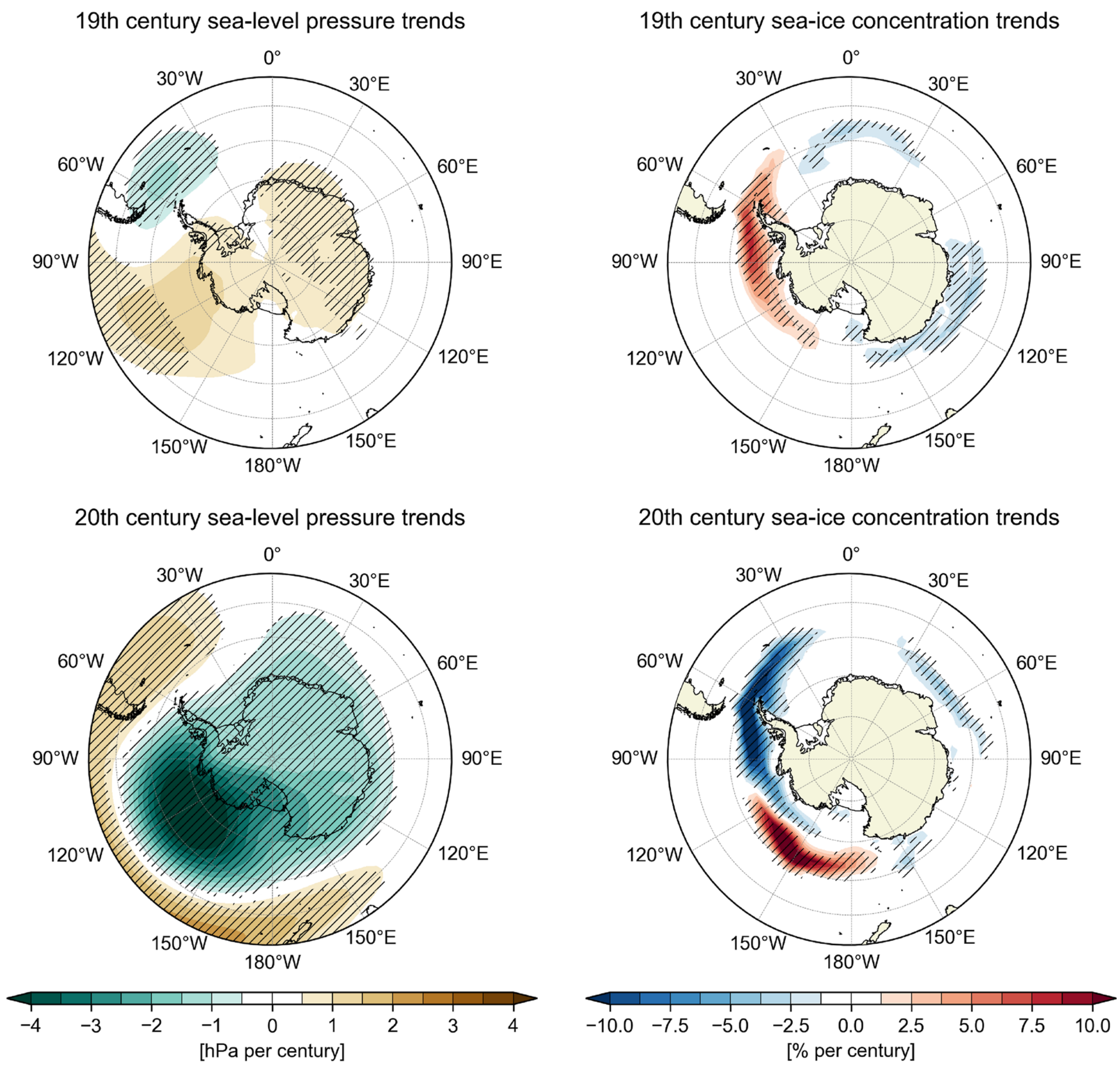

Figure 2. Reconstructed 19th (top) and 20th (bottom) century trends of sea-level pressure (left; in hPa per century) and sea-ice concentration (right; in % per century) in our DA-based reconstruction. Stippling indicates statistically significant trends (95% confidence), which result from a method taking into account the false-discovery rate (FDR) (Benjamini & Hochberg, 1995).

action is located off the Amundsen Sea coast (Hosking et al., 2013; Raphael et al., 2016), indicated in two recent reconstructions (Dalaiden et al., 2021; O'Connor et al., 2021). Southerly winds associated with a deeper Amundsen Sea Low bring cold air from Antarctica to the Ross Sea and push the sea ice northward, resulting in a higher sea-ice extent in the Ross Sea. The opposite situation occurs in the Weddell Sea and part of the Bellingshausen Sea as more northerly winds reduce the sea-ice extent when the Amundsen Sea Low is stronger.

3.3. Comparison With Climate Model Results

Climate models are generally not able to reproduce the observed trends in Antarctic sea-ice extent over the past half century, most of them simulating a large decrease in contrast to the relatively stable observed values (Roach et al., 2022). A similar situation is obtained here for the 20th century, with a moderate decrease in both our reconstruction and in Fogt22 that is a factor 5 smaller than the mean of the simulations covering the past centuries but still marginally in the range provided by the ensemble (Table 1). However, part of this apparent agreement can be due to models that might strongly overestimate the variability of the sea-ice extent, providing a wide range of model results (Roach et al., 2022; Zunz et al., 2013). The models tend to simulate a retreat of sea ice in most sectors, although an increase in sea-ice concentration can also be found at some locations (Figure S7

10.1029/2023GL104666

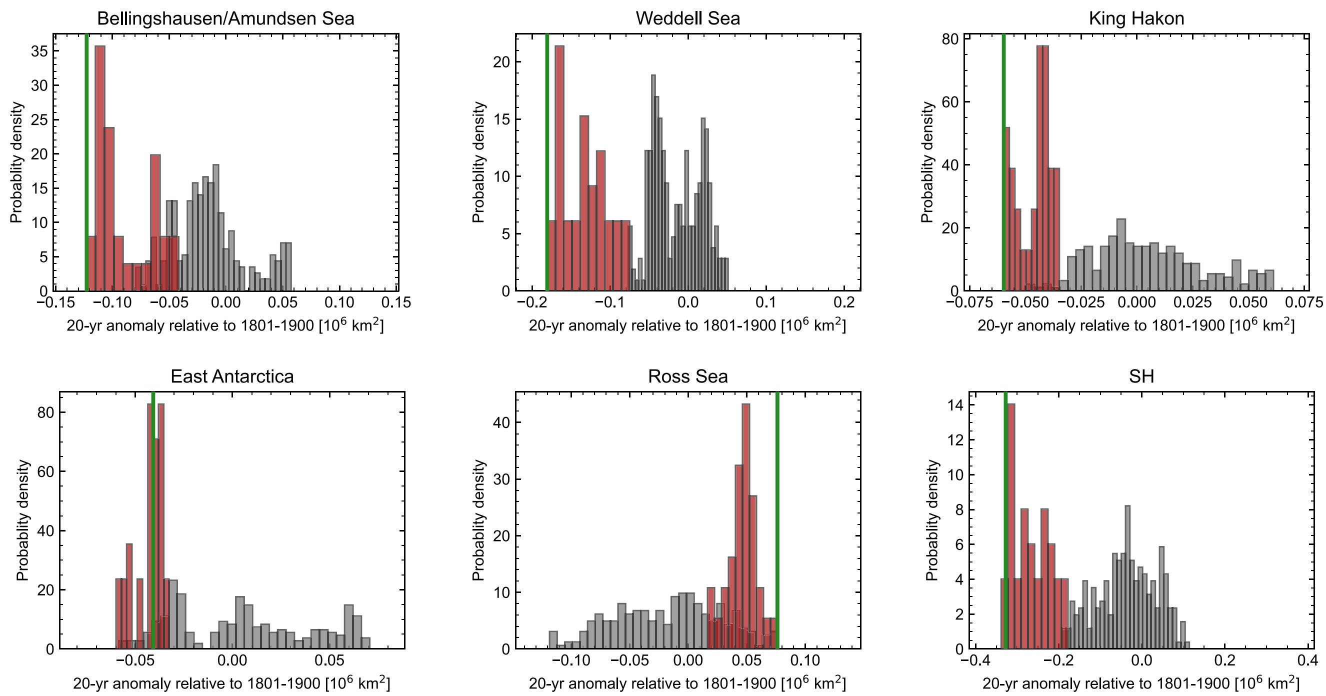

Figure 3. Distributions of probability density of reconstructed 20-year anomalies of sea-ice extent for the five Antarctic regions and Antarctic as a whole. Anomalies are computed over 1801–1900 CE period. Gray bars correspond to the 1700–1949 CE period while red bars represent the 1950–2000 CE period. Green vertical lines correspond to the 1980–2000 CE anomalies.

in Supporting Information S1). For instance, the 12 members of the CESM1 display a decreasing trend that is much larger than the reconstruction, showing that for this model, internal variability cannot compensate for the large retreat imposed by the forcing (Table 1). On a regional scale, the simulated trends of the sea-ice extent in the Weddell and Bellingshausen-Amundsen sectors are similar to what we obtain in our reconstruction (Table 1). For the East Antarctica and King Hakon sectors, a large melting is also obtained in the models but the low skill of our reconstruction there prevents any robust comparison. Nevertheless, a clear disagreement is obtained in the Ross Sea, with no model being able to reproduce the positive trend in sea-ice extent associated with the stronger southerly winds reconstructed for this sector.

4. Discussion and Conclusions

Our reconstruction indicates a decreasing trend in the Weddell Sea over the 20th century of 0.259 ± 0.031 million km^2, with the largest decrease occurring before the 1960s. This contrasts with the relatively stable sea-ice extent over the preceding 200 years. As a consequence, the sea-ice extent of the Weddell Sea at the end of the 20th century is lower in our reconstruction than any other period between 1700 CE and 2000 CE (Figure 3). Associating a significance level to this value is difficult because of the uncertainty in the reconstruction and the complex distribution of the anomalies. However, the sea-ice extent averaged over 1980–2000 CE is lower than the mean over 1800–1900 CE by more than five standard deviations of overlapping 20-yr averages over that period, showing the robustness of the signal. This also suggests that the minimum values observed in the area over the past few years (Turner et al., 2022) are exceptional in the context of the past 300 years.

The sea ice reduction over the Weddell Sea drives a decrease of the same magnitude of the sea-ice extent over the whole Southern Ocean, leading also to a low value at the end of the 20th century compared to the preceding centuries. In our reconstruction, this similar magnitude of the trend for the Weddell Sea and the whole Southern Ocean is due to a strong compensation between a positive trend in the Ross Sector and a negative trend in the Bellingshausen-Amundsen Sector. This compensation is caused by the intensification of cyclonic circulation in the eastern Pacific sector, associated with a deepening of the Amundsen Sea low over the 20th century.

Despite regional variations in the sea ice trends present in some model simulations, models tend to simulate a larger and more spatially homogeneous retreat than our reconstruction. This is particularly the case in the prior used in these reconstructions. All the ensemble members display a largely uniform sea-ice cover decrease over the 20th century, despite variations in atmospheric circulation changes between the ensemble members (Figure S8 in Supporting Information S1). Specifically, the models are not able to reproduce the reconstructed increasing trend in the Ross sector, the region where the main disagreement between models and observed trends over the past decades occur (M. M. Holland et al., 2017; Hobbs et al., 2015). Several processes could be responsible of these model biases, including a misrepresentation of ocean–sea-ice feedback (Lecomte et al., 2017), of the impact of the meltwater flux (Rye et al., 2020) and of the effect of the winds (Blanchard-Wrigglesworth et al., 2021; X. Zhang et al., 2021; Sun & Eisenman, 2021). Although we did not make specific diagnostics on the sea-ice budget to quantify the role of those processes, our results are consistent with an underestimation of the influence of the wind changes in models as the reconstructed increase in southerly winds likely contributed to the annual mean expansion of the sea-ice extent in the Ross Sea (Blanchard-Wrigglesworth et al., 2021).

Discerning the contributions of the internal and forced variability on the observed sea ice changes is critical to provide accurate projections for the coming decades. Our findings underscore the key role of winds in the sea ice changes. Yet, several studies have identified a clear impact of the stratospheric ozone depletion and of the increase in greenhouse gases in the observed trends in the SAM and the related Amundsen Sea Low (Dalaiden et al., 2022; England et al., 2018; Thompson et al., 2011), which play a central role in the reconstructed sea ice changes. However, albeit our reconstructions provide skilful estimates over a majority of the Southern Ocean, a comprehensive circumpolar perspective requires additional information in East Antarctica, in particular in the Indian sector. Such circumpolar reconstructions could ultimately be used for placing the recent Antarctic sea-ice extent minima (Turner et al., 2022) within a broader historical context. Additionally, quantifying the relative contributions of internal and forced variability would require a clear identification of the fingerprint of the response to anthropogenic forcing, which is still a challenge because of the current biases in climate model results (Roach et al., 2022). Therefore, future work is needed to extend the paleo-based reconstruction to East Antarctica and improve climate models to be able to estimate the contributions of internal and forced variability in recent sea ice changes.

Data Availability Statement

Our reconstructions of sea ice and winds are publicly available on Zenodo (Dalaiden et al., 2023). Sea-ice concentration data set from the NSIDC is freely available (NSIDC, 2023). Regional reconstructions of sea-ice extent of Fogt et al. (2022) is publicly available (Fogt et al., 2023). The Marshall index is stored on the British Antarctic Survey website (G. Marshall, 2003). The SAM reconstruction of Dätwyler, Grosjean, et al. (2019) is available via the NOAA website (Dätwyler, Neukom, et al., 2019). The ERA5 atmospheric reanalysis (Hersbach et al., 2020a) was downloaded from the Copernicus Climate Change Service (C3S) Climate Data Store (Hersbach et al., 2020b). PMIP3 model outputs can be downloaded on the esgf website (PMIP, 2018). The last millennium large ensemble of CESM1 (Otto-Bliesner et al., 2015b) and iCESM1 (Brady et al., 2019; Stevenson et al., 2019) is freely accessible (Otto-Bliesner et al., 2015a). The Global Meteorological Forcing Data set for land surface modeling version 2 (Sheffield et al., 2006a) used for calibrating the TRW PSMs can be freely downloaded (Sheffield et al., 2006b). $\delta^{18}O$ and snow accumulation can be accessed via the NOAA World Data Center for Paleoclimatology (Stenni et al., 2017b), British Antarctic Survey website (Thomas et al., 2017b) and the tree-ring width records are available on *figshare* (Emile-Geay et al., 2017b). The database of Na+ ice-core records from Thomas et al. (2022) is stored at the UK Polar Data Centre (Thomas, et al., 2017c). The South Orkney Fast-Ice Series (SOFI) of Murphy et al. (2014a) is stored on the British Antarctic Survey website (Murphy et al., 2014b).

Acknowledgments

We would like to thank the ice core and Pages2k community for gathering all the proxy records for reconstructing the climate over the past centuries. We acknowledge the World Climate Research Programme's Working Group on Coupled Modelling, which is responsible for CMIP. For CMIP the US Department of Energy's Program for Climate Model Diagnosis and Intercomparison provides coordinating support and led development of software infrastructure in partnership with the Global Organization for Earth System Science Portals. We also would like to thank the NCAR and ECWMF for providing their isotope-enable model simulations and atmospheric reanalysis. QD is a Research Fellow within the F.R.S.-FNRS (Belgium). HG is a Research Director within the F.R.S.-FNRS (Belgium). This work was performed in the framework of the PDR project T.0101.22 "Role of WINDS and oceanic interactions on Sea ice Changes in the SOuthern Ocean over the Past millennium (WindSCOOP)" of the FRS-FNRS. And supported by the Belgian Research Action through Interdisciplinary Networks (BRAIN-be) from Belgian Science Policy Office in the framework of the project "East Antarctic surface mass balance in the Anthropocene: observations and multiscale modelling (Mass2Ant)" (Contrat n° BR/165/A2/Mass2Ant). Finally, we would like to thank the two anonymous reviewers for their comments on the study that undoubtedly improve the quality of the manuscript.

References

Abram, N. J., Thomas, E. R., McConnell, J. R., Mulvaney, R., Bracegirdle, T. J., Sime, L. C., & Aristarain, A. J. (2010). Ice core evidence for a 20th century decline of sea ice in the Bellingshausen Sea, Antarctica. *Journal of Geophysical Research*, *115*(23), 1–9. https://doi.org/10.1029/2010JD014644

Benjamini, Y., & Hochberg, Y. (1995). Controlling the false discovery rate: A practical and powerful approach to multiple testing. *Journal of the Royal Statistical Society: Series B*, *57*(1), 289–300. https://doi.org/10.1111/j.2517-6161.1995.tb02031.x

Blanchard-Wrigglesworth, E., Roach, L. A., Donohoe, A., & Ding, Q. (2021). Impact of winds and southern ocean ssts on antarctic sea ice trends and variability. *Journal of Climate*, *34*(3), 949–965. https://doi.org/10.1175/JCLI-D-20-0386.1

Brady, E., Stevenson, S., Bailey, D., Liu, Z., Noone, D., Nusbaumer, J., et al. (2019). The connected isotopic water cycle in the community Earth system model version 1. *Journal of Advances in Modeling Earth Systems*, *11*(8), 2547–2566. https://doi.org/10.1029/2019MS001663

Brennan, M. K., Hakim, G. J., & Blanchard-Wrigglesworth, E. (2020). Arctic sea-ice variability during the instrumental era. *Geophysical Research Letters*, *47*(7), 1–9. https://doi.org/10.1029/2019GL086843

Caillet, J., Jourdain, N. C., Mathiot, P., Hellmer, H. H., & Mouginot, J. (2023). Drivers and reversibility of abrupt ocean state transitions in the Amundsen Sea, Antarctica. *Journal of Geophysical Research: Oceans*, *128*(1), e2022JC018929. https://doi.org/10.1029/2022JC018929

Crosta, X., Etourneau, J., Orme, L. C., Dalaiden, Q., Campagne, P., Swingedouw, D., et al. (2021). Multi-decadal trends in Antarctic sea-ice extent driven by ENSO–SAM over the last 2,000 years. *Nature Geoscience*, *14*(3), 156–160. https://doi.org/10.1038/s41561-021-00697-1

Curran, M. A., Van Ommen, T. D., Morgan, V. I., Phillips, K. L., & Palmer, A. S. (2003). Ice core evidence for Antarctic sea ice decline since the 1950s. *Science*, *302*(5648), 1203–1206. https://doi.org/10.1126/science.1087888

Dalaiden, Q., Goosse, H., Rezsöhazy, J., & Thomas, E. R. (2021). Reconstructing atmospheric circulation and sea-ice extent in the west Antarctic over the past 200 years using data assimilation. *Climate Dynamics*, *57*(11), 3479–3503. https://doi.org/10.1007/s00382-021-05879-6

Dalaiden, Q., Rezsohazy, J., Goosse, H., Thomas, E., Vladimirova, D., & Tetzner, D. (2023). Reconstructed sea ice and winds [Dataset]. Zenodo. https://doi.org/10.5281/zenodo.7966209

Dalaiden, Q., Schurer, A. P., Kirchmeier-young, M. C., Goosse, H., & Hegerl, G. C. (2022). West Antarctic surface climate changes since the mid-20th century driven by anthropogenic forcing geophysical research letters. *Geophysical Research Letters*, *49*(16), e2022GL099543. https://doi.org/10.1029/2022GL099543

Dätwyler, C., Grosjean, M., Steiger, N. J., & Neukom, R. (2019). Teleconnections and relationship between ENSO and SAM in reconstructions and models over the past millennium. In *Climate of the past discussions* (pp. 1–20). https://doi.org/10.5194/cp-2019-110

Dätwyler, C., Neukom, R., Abram, N. J., Gallant, A. J., Grosjean, M., Jacques-Coper, M., et al. (2018). Teleconnection stationarity, variability and trends of the Southern Annular Mode (SAM) during the last millennium. *Climate Dynamics*, *51*(5), 1–19. https://doi.org/10.1007/s00382-017-4015-0

Dätwyler, C., Neukom, R., Abram, N. J., Gallant, A. J., Grosjean, M., Jacques-Coper, M., et al. (2019). Paleo-based southern annular mode index [Dataset]. NCEI. Retrieved from https://www.ncei.noaa.gov/pub/data/paleo/reconstructions/datwyler2017/readme-datwyler2017.txt

De La Mare, W. K. (1997). Abrupt mid-twentieth-century decline in Antarctic sea-ice extent from whaling records. *Nature*, *389*(6646), 57–60. https://doi.org/10.1038/37956

Dubinkina, S., Goosse, H., Sallaz-Damaz, Y., Crespin, E., & Crucifix, M. (2011). Testing a particle filter to reconstruct climate changes over the past centuries. *International Journal of Bifurcation and Chaos*, *21*(12), 3611–3618. https://doi.org/10.1142/S0218127411030763

Edinburgh, T., & Day, J. J. (2016). Estimating the extent of Antarctic summer sea ice during the Heroic Age of Antarctic exploration. *The Cryosphere*, *10*(6), 2721–2730. https://doi.org/10.5194/tc-10-2721-2016

Emile-Geay, J., McKay, N. P., Kaufman, D. S., von Gunten, L., Wang, J., Anchukaitis, K. J., et al. (2017a). A global multiproxy database for temperature reconstructions of the Common Era. *Scientific Data*, *4*(1), 170088. https://doi.org/10.1038/sdata.2017.88

Emile-Geay, J., McKay, N. P., Kaufman, D. S., von Gunten, L., Wang, J., Anchukaitis, K. J., et al. (2017b). A global multiproxy database for temperature reconstructions of the Common Era [Dataset]. figshare. Retrieved from https://springernature.figshare.com/collections/A_global_multiproxy_database_for_temperature_reconstructions_of_the_Common_Era/3285353

England, M., Polvani, L., & Sun, L. (2018). Contrasting the Antarctic and Arctic atmospheric responses to projected sea ice loss in the late twenty-first century. *Journal of Climate*, *31*(16), 6353–6370. https://doi.org/10.1175/JCLI-D-17-0666.1

Evans, M. N., Tolwinski-Ward, S. E., Thompson, D. M., & Anchukaitis, K. J. (2013). Applications of proxy system modeling in high resolution paleoclimatology. *Quaternary Science Reviews*, *76*, 16–28. https://doi.org/10.1016/j.quascirev.2013.05.024

Fan, T., Deser, C., & Schneider, D. (2014). Recent Antarctic sea ice trends in the context of Southern Ocean surface climate variations since 1950. *Geophysical Research Letters*, *41*(7), 2419–2426. https://doi.org/10.1002/2014GL059239

Fogt, R. L., & Connolly, C. J. (2021). Extratropical southern hemisphere synchronous pressure variability in the early twentieth century. *Journal of Climate*, *34*(14), 5795–5811. https://doi.org/10.1175/JCLI-D-20-0498.1

Fogt, R. L., Sleinkofer, A. M., Raphael, M. N., & Handcock, M. S. (2022). A regime shift in seasonal total Antarctic sea ice extent in the twentieth century. *Nature Climate Change*, *12*(1), 54–62. https://doi.org/10.1038/s41558-021-01254-9

Fogt, R. L., Sleinkofer, A. M., Raphael, M. N., & Handcock, M. S. (2023). Instrumental-based sea-ice extent reconstruction over the 20th century [Dataset]. figshare. Retrieved from https://figshare.com/collections/Antarctic_Sea_Ice_Reconstructions/5709767/1

Goosse, H., Crespin, E., de Montety, A., Mann, M. E., Renssen, H., & Timmermann, A. (2010). Reconstructing surface temperature changes over the past 600 years using climate model simulations with data assimilation. *Journal of Geophysical Research*, *115*(D9), D09108. https://doi.org/10.1029/2009JD012737

Goosse, H., Lefebvre, W., de Montety, A., Crespin, E., & Orsi, A. H. (2009). Consistent past half-century trends in the atmosphere, the sea ice and the ocean at high southern latitudes. *Climate Dynamics*, *33*(7–8), 999–1016. https://doi.org/10.1007/s00382-008-0500-9

Hakim, G. J., Emile-Geay, J., Steig, E. J., Noone, D., Anderson, D. M., Tardif, R., et al. (2016). The last millennium climate reanalysis project: Framework and first results. *Journal of Geophysical Research*, *121*(12), 6745–6764. https://doi.org/10.1002/2016JD024751

Hersbach, H., Bell, B., Berrisford, P., Hirahara, S., Horányi, A., Muñoz-Sabater, J., et al. (2020a). The ERA5 global reanalysis. *Quarterly Journal of the Royal Meteorological Society*, *146*(730), 1999–2049. https://doi.org/10.1002/qj.3803

Hersbach, H., Bell, B., Berrisford, P., Hirahara, S., Horányi, A., Muñoz-Sabater, J., et al. (2020b). ERA5 hourly data on pressure levels from 1940 to present [Dataset]. Copernicus Climate Change Service (C3S) Climate Data Store (CDS). Retrieved from https://cds.climate.copernicus.eu/cdsapp#!/dataset/reanalysis-era5-single-levels?tab=overview

Hobbs, W. R., Bindoff, N. L., & Raphael, M. N. (2015). New perspectives on observed and simulated Antarctic sea ice extent trends using optimal fingerprinting techniques. *Journal of Climate*, *28*(4), 1543–1560. https://doi.org/10.1175/JCLI-D-14-00367.1

Hobbs, W. R., Massom, R., Stammerjohn, S., Reid, P., Williams, G., & Meier, W. (2016). A review of recent changes in Southern Ocean sea ice, their drivers and forcings. *Global and Planetary Change*, *143*, 228–250. https://doi.org/10.1016/j.gloplacha.2016.06.008

Holland, M. M., Landrum, L., Kostov, Y., & Marshall, J. (2017). Sensitivity of Antarctic sea ice to the Southern Annular Mode in coupled climate models. *Climate Dynamics*, *49*(5–6), 1813–1831. https://doi.org/10.1007/s00382-016-3424-9

Holland, P. R., & Kwok, R. (2012). Wind-driven trends in Antarctic sea-ice drift. *Nature Geoscience*, *5*(12), 872–875. https://doi.org/10.1038/ngeo1627

Hosking, J. S., Orr, A., Marshall, G. J., Turner, J., & Phillips, T. (2013). The influence of the Amundsen-Bellingshausen seas low on the climate of West Antarctica and its representation in coupled climate model simulations. *Journal of Climate*, *26*(17), 6633–6648. https://doi.org/10.1175/JCLI-D-12-00813.1

Klein, F., Abram, N. J., Curran, M. A. J., Goosse, H., Goursaud, S., Masson-Delmotte, V., et al. (2019). Assessing the robustness of Antarctic temperature reconstructions over the past two millennia using pseudoproxy and data assimilation experiments. *Climate of the Past*, *15*, 661–684. https://doi.org/10.5194/cp-2018-90

Kusahara, K., Williams, G. D., Massom, R., Reid, P., & Hasumi, H. (2019). Spatiotemporal dependence of Antarctic sea ice variability to dynamic and thermodynamic forcing: A coupled ocean–sea ice model study. *Climate Dynamics*, *52*(7), 3791–3807. https://doi.org/10.1007/s00382-018-4348-3

Landrum, L. L., Holland, M. M., Raphael, M. N., & Polvani, L. M. (2017). Stratospheric ozone depletion: An unlikely driver of the regional trends in Antarctic Sea Ice in austral fall in the late twentieth century. *Geophysical Research Letters*, *44*(21), 11062–11070. https://doi.org/10.1002/2017GL075618

Lecomte, O., Goosse, H., Fichefet, T., De Lavergne, C., Barthélemy, A., & Zunz, V. (2017). Vertical ocean heat redistribution sustaining sea-ice concentration trends in the Ross Sea. *Nature Communications*, *8*(1), 258. https://doi.org/10.1038/s41467-017-00347-4

Lefebvre, W., & Goosse, H. (2005). Influence of the southern annular mode on the sea ice-ocean system: The role of the thermal and mechanical forcing. *Ocean Science*, *1*(3), 145–157. https://doi.org/10.5194/os-1-145-2005

Legrand, M., & Mayewski, P. (1997). Glaciochemistry of polar ice cores: A review. *Reviews of Geophysics*, *35*(3), 219–243. https://doi.org/10.1029/96RG03527

Marshall, G. (2003). Southern annular mode index from Gareth Marshall [Dataset]. Legacy. Retrieved from https://legacy.bas.ac.uk/met/gjma/sam.html

Marshall, G. J. (2003). Trends in the southern annular mode from observations and reanalyses. *Journal of Climate*, *16*(1999), 4134–4143. https://doi.org/10.1175/1520-0442(2003)016⟨4134:TITSAM⟩2.0.CO;2

Matsikaris, A., Widmann, M., & Jungclaus, J. (2015). On-line and off-line data assimilation in palaeoclimatology: A case study. *Climate of the Past*, *11*(1), 81–93. https://doi.org/10.5194/cp-11-81-2015

Mayewski, P. A., Carleton, A. M., Birkel, S. D., Dixon, D., Kurbatov, A. V., Korotkikh, E., et al. (2017). Ice core and climate reanalysis analogs to predict Antarctic and Southern Hemisphere climate changes. *Quaternary Science Reviews*, *155*, 50–66. https://doi.org/10.1016/j.quascirev.2016.11.017

Medley, B., McConnell, J. R., Neumann, T. A., Reijmer, C. H., Chellman, N., Sigl, M., & Kipfstuhl, S. (2018). Temperature and snowfall in western Queen Maud Land increasing faster than climate model projections. *Geophysical Research Letters*, *45*(3), 1472–1480. https://doi.org/10.1002/2017GL075992

Münch, T., & Laepple, T. (2018). What climate signal is contained in decadal - To centennial-scale isotope variations from Antarctic ice cores? *Climate of the Past*, *14*(12), 2053–2070. https://doi.org/10.5194/cp-14-2053-2018

Murphy, E. J., Clarke, A., Abram, N. J., & Turner, J. (2014a). Variability of sea-ice in the northern Weddell sea during the 20th century. *Journal of Geophysical Research: Oceans*, *119*(7), 4549–4572. https://doi.org/10.1002/2013JC009511

Murphy, E. J., Clarke, A., Abram, N. J., & Turner, J. (2014b). Variability of sea-ice in the northern Weddell Sea during the 20th century [Dataset]. British and American Studies. Retrieved from https://data.bas.ac.uk/full-record.php?id=GB/NERC/BAS/PDC/00802

NSIDC. (2023). Satelitte sea-ice concentration product [Dataset]. NSIDC. Retrieved from https://nsidc.org/data/NSIDC-0051/versions/1

O'Connor, G. K., Steig, E. J., & Hakim, G. J. (2021). Strengthening Southern Hemisphere westerlies and Amundsen sea low deepening over the 20th century revealed by proxy-data assimilation. *Geophysical Research Letters*, *48*(24), e2021GL095999. https://doi.org/10.1029/2021gl095999

Okazaki, A., Miyoshi, T., Yoshimura, K., Greybush, S. J., & Zhang, F. (2021). Revisiting online and offline data assimilation comparison for paleoclimate reconstruction: An idealized OSSE study. *Journal of Geophysical Research: Atmospheres*, *126*(16), e2020JD034214. https://doi.org/10.1029/2020JD034214

Otto-Bliesner, B. L., Brady, E. C., Fasullo, J., Jahn, A., Landrum, L., Stevenson, S., et al. (2015b). Climate variability and change since 850 CE: An ensemble approach with the community Earth system model. *Bulletin of the American Meteorological Society*, *97*(5), 735–754. https://doi.org/10.1175/bams-d-14-00233.1

Otto-Bliesner, B. L., Brady, E. C., Fasullo, J., Jahn, A., Landrum, L., Stevenson, S., et al. (2015a). CESM1 last millennium large ensemble [Dataset]. Earthsystemgrid. Retrieved from https://www.earthsystemgrid.org/dataset/ucar.cgd.ccsm4.cesmLME.html

PAGES2k Consortium, Ahmed, M., Anchukaitis, K. J., Asrat, A., Borgaonkar, H. P., Braida, M., & Consortium, P. K. (2013). Continental-scale temperature variability during the past two millennia. *Nature Geoscience*, *6*(5), 339–346. https://doi.org/10.1038/ngeo1797

Parkinson, C. L. (2019). A 40-y record reveals gradual Antarctic sea ice increases followed by decreases at rates far exceeding the rates seen in the Arctic. *Proceedings of the National Academy of Sciences of the United States of America*, *116*(29), 14414–14423. https://doi.org/10.1073/pnas.1906556116

PMIP. (2018). PMIP3 model outputs [Dataset]. ESGF. Retrieved from https://esgf-index1.ceda.ac.uk/projects/esgf-ceda/

Polvani, L. M., Banerjee, A., Chemke, R., Doddridge, E. W., Ferreira, D., Gnanadesikan, A., et al. (2021). Interannual SAM modulation of antarctic sea ice extent does not account for its long-term trends, pointing to a limited role for ozone depletion. *Geophysical Research Letters*, *48*(21), 1–10. https://doi.org/10.1029/2021GL094871

Polvani, L. M., & Smith, K. L. (2013). Can natural variability explain observed Antarctic sea ice trends? New modeling evidence from CMIP5. *Geophysical Research Letters*, *40*(12), 3195–3199. https://doi.org/10.1002/grl.50578

Raphael, M. N., & Hobbs, W. (2014). The influence of the large-scale atmospheric circulation on antarctic sea ice during ice advance and retreat seasons. *Geophysical Research Letters*, *41*(14), 5037–5045. https://doi.org/10.1002/2014GL060365

Raphael, M. N., Marshall, G. J., Turner, J., Fogt, R. L., Schneider, D., Dixon, D. A., et al. (2016). The Amundsen sea low: Variability, change, and impact on Antarctic climate. *Bulletin of the American Meteorological Society*, *97*(1), 111–121. https://doi.org/10.1175/BAMS-D-14-00018.1

Rezsöhazy, J., Dalaiden, Q., Klein, F., Goosse, H., & Guiot, J. (2022). Using a process-based dendroclimatic proxy system model in a data assimilation framework: A test case in the southern hemisphere over the past centuries. *Climate of the Past*, *18*(9), 2093–2115. https://doi.org/10.5194/cp-18-2093-2022

Roach, L. A., Dörr, J., Holmes, C. R., Massonnet, F., Blockley, E. W., Notz, D., et al. (2020). Antarctic sea ice area in CMIP6. *Geophysical Research Letters*, *47*(9), 1–24. https://doi.org/10.1029/2019GL086729

Roach, L. A., Eisenman, I., Wagner, T. J., Blanchard-Wrigglesworth, E., & Bitz, C. M. (2022). Asymmetry in the seasonal cycle of Antarctic sea ice due to insolation. *Nature Geoscience*, *15*(4), 277–281. https://doi.org/10.1038/s41561-022-00913-6

Rye, C. D., Marshall, J., Kelley, M., Russell, G., Nazarenko, L. S., Kostov, Y., et al. (2020). Antarctic glacial melt as a driver of recent southern ocean climate trends. *Geophysical Research Letters*, *47*(11), 0–3. https://doi.org/10.1029/2019GL086892

Schneider, D. P., & Deser, C. (2018). Tropically driven and externally forced patterns of Antarctic sea ice change: Reconciling observed and modeled trends. *Climate Dynamics*, *50*(11–12), 4599–4618. https://doi.org/10.1007/s00382-017-3893-5

Sheffield, J., Goteti, G., & Wood, E. F. (2006a). Development of a 50-yr high-resolution global dataset of meteorological forcings for land surface modeling. *Journal of Climate*, *19*(12), 3088–3111. https://doi.org/10.1175/jcli3790.1

Sheffield, J., Goteti, G., & Wood, E. F. (2006b). Development of a 50-yr high-resolution global dataset of meteorological forcings for land surface modeling [Dataset]. SOTON. Retrieved from https://hydrology.soton.ac.uk/data/pgf/v2/

Stammerjohn, S. E., Martinson, D. G., Smith, R. C., Yuan, X., & Rind, D. (2008). Trends in antarctic annual sea ice retreat and advance and their relation to El Niño–Southern Oscillation and southern annular mode variability. *Journal of Geophysical Research*, *113*(C3), C03S90. https://doi.org/10.1029/2007JC004269

Steiger, N. J., Steig, E. J., Dee, S. G., Roe, G. H., & Hakim, G. J. (2017). Climate reconstruction using data assimilation of water isotope ratios from ice cores. *Journal of Geophysical Research: Atmospheres*, *122*(3), 1545–1568. https://doi.org/10.1002/2016JD026011

Stenni, B., Curran, M. A., Abram, N. J., Orsi, A., Goursaud, S., Masson-Delmotte, V., et al. (2017b). Regional Antarctic snow accumulation over the past 1000 years [Dataset]. NCEI. Retrieved from https://www.ncei.noaa.gov/access/paleo-search/study/22589

Stenni, B., Curran, M. A., Abram, N. J., Orsi, A., Goursaud, S., Masson-Delmotte, V., et al. (2017a). Antarctic climate variability on regional and continental scales over the last 2000 years. *Climate of the Past*, *13*(11), 1609–1634. https://doi.org/10.5194/cp-13-1609-2017

Stevenson, S., Capotondi, A., Fasullo, J., & Otto-Bliesner, B. (2019). Forced changes to twentieth century ENSO diversity in a last Millennium context. *Climate Dynamics*, *52*(12), 7359–7374. https://doi.org/10.1007/s00382-017-3573-5

Sun, S., & Eisenman, I. (2021). Observed Antarctic sea ice expansion reproduced in a climate model after correcting biases in sea ice drift velocity. *Nature Communications*, *12*(1), 1060. https://doi.org/10.1038/s41467-021-21412-z

Thomas, E. R., & Abram, N. J. (2016). Ice core reconstruction of sea ice change in the Amundsen-Ross Seas since 1702 A.D. *Geophysical Research Letters*, *43*(10), 5309–5317. https://doi.org/10.1002/2016GL068130

Thomas, E. R., Allen, C. S., Etourneau, J., King, A. C. F., Severi, M., Winton, V. H. L., et al. (2019). Antarctic sea ice proxies from marine and ice core archives suitable for reconstructing sea ice over the past 2000 years. *Geosciences*, *9*(12), 1–33. https://doi.org/10.3390/geosciences9120506

Thomas, E. R., Melchior Van Wessem, J., Roberts, J., Isaksson, E., Schlosser, E., Fudge, T. J., et al. (2017b). Regional Antarctic snow accumulation over the past 1000 years [Dataset]. NCEI. Retrieved from https://www.ncei.noaa.gov/access/paleo-search/study/22589

Thomas, E. R., Melchior Van Wessem, J., Roberts, J., Isaksson, E., Schlosser, E., Fudge, T. J., et al. (2017a). Regional Antarctic snow accumulation over the past 1000 years. *Climate of the Past*, *13*(11), 1491–1513. https://doi.org/10.5194/cp-13-1491-2017

Thomas, E. R., Vladimirova, D. O., Tetzner, D. R., Emanuelsson, B. D., Chellman, N., Dixon, D. A., et al. (2017c). Ice core chemistry database: An Antarctic compilation of sodium and sulphate records spanning the past 2000 years [Dataset]. Earth System Science Data. https://doi.org/10.5285/9E0ED16E-F2AB-4372-8DF3-FDE7E388C9A7

Thomas, E. R., Vladimirova, D. O., Tetzner, D. R., Emanuelsson, B. D., Chellman, N., Dixon, D. A., et al. (2022). Ice core chemistry database: An antarctic compilation of sodium and sulphate records spanning the past 2000 years. In *Earth system science data discussions* (pp. 1–20). https://doi.org/10.5194/essd-2022-368

Thompson, D. W. J., Solomon, S., Kushner, P. J., England, M. H., Grise, K. M., & Karoly, D. J. (2011). Signatures of the Antarctic ozone hole in Southern Hemisphere surface climate change. *Nature Geoscience*, *4*(11), 741–749. https://doi.org/10.1038/ngeo1296

Titchner, H. A., & Rayner, N. A. (2014). The met office Hadley centre sea ice and sea surface temperature data set, version 2: 1. Sea ice concentrations. *Journal of Geophysical Research: Atmospheres*, *119*(6), 2864–2889. https://doi.org/10.1002/2013JD020316

Turner, J., Holmes, C., Caton Harrison, T., Phillips, T., Jena, B., Reeves-Francois, T., et al. (2022). Record low Antarctic sea ice cover in February 2022. *Geophysical Research Letters*, *49*(12), e2022GL098904. https://doi.org/10.1029/2022gl098904

van Leeuwen, P. J. (2009). Particle filtering in geophysical systems. *Monthly Weather Review*, *137*(12), 4089–4114. https://doi.org/10.1175/2009MWR2835.1

Widmann, M., Goosse, H., Van Der Schrier, G., Schnur, R., & Barkmeijer, J. (2010). Using data assimilation to study extratropical Northern Hemisphere climate over the last millennium. *Climate of the Past*, *6*(5), 627–644. https://doi.org/10.5194/cp-6-627-2010

Zhang, L., Delworth, T. L., Cooke, W., & Yang, X. (2019). Natural variability of southern ocean convection as a driver of observed climate trends. *Nature Climate Change*, *9*(1), 59–65. https://doi.org/10.1038/s41558-018-0350-3

Zhang, X., Deser, C., & Sun, L. (2021). Is there a tropical response to recent observed southern ocean cooling? *Geophysical Research Letters*, *48*(5), e2020GL091235. https://doi.org/10.1029/2020GL091235

Zunz, V., Goosse, H., & Massonnet, F. (2013). How does internal variability influence the ability of CMIP5 models to reproduce the recent trend in Southern Ocean sea ice extent? *The Cryosphere*, *7*(2), 451–468. https://doi.org/10.5194/tc-7-451-2013